Organized Nanostructured Complexes of Inorganic Clusters and Surfactants That Exhibit Thermal Solid-State Transformations

Franck Camerel, Markus Antonietti, and Charl F. J. Faul*[a]

Abstract: Facile organization of the inorganic crown-shaped $[Ni_3P_3S_{12}]^{3-}$ ion (**1**) into room-temperature liquid-crystalline materials by complexation with double-tail ammonium surfactants is achieved by the ionic self-assembly (ISA) route. Small-angle X-ray diffraction, UV/Vis spectroscopy, and ^{31}P NMR analyses reveal that these complexes show an interesting solid-state structure transition. Upon heating, the inorganic crown species polymerizes to the inorganic polyelectrolyte $^1_\infty[NiPS_4]^-$. This structural transition is reversible, and involves a solvent/dissolution cycle. The facile preparation and facile optional induction of phase and structural changes make these complexes candidates for a number of applications in which cooperative, metastable switching with sufficient contrast of optical and solid-state properties is required.

Keywords: ionic self-assembly · liquid crystals · nanostructures · supramolecular chemistry · surfactants

Introduction

Self-assembly, a process well known to nature[1, 2] has provided a way to produce organized matter with complex supramolecular architectures.[3–6] In the search for supramolecular functional materials the aim is that the molecular information coded within the structure of the tectonic units should induce controlled organization. The specific functions of the material should then, ideally, be a direct result of the formed structure[7, 8] and, in the case of dynamic devices, should be externally triggered (by light, pressure, temperature etc.) to produce reversible changes.

Recently, a facile route for the production of highly organized supramolecular materials from a variety of charged building blocks by complexation with surfactants was introduced.[9] Unlike the well-known routes of supramolecular synthesis (such as H-bonding interactions,[10] metal-ion coordination interactions,[11] etc.), the ionic self-assembly (ISA) process uses electrostatic interactions between charged surfactants and oppositely charged oligoelectrolytic species as the primary interaction, and hydrophobic and $\pi-\pi$ interactions as secondary motifs to promote self-organization. By introduction of double-tail surfactant species, and thereby increasing the number of alkyl groups within the materials, it is also possible to produce soft materials from very rigid tectonic units, which show thermotropic liquid-crystalline behavior.[12] This principle of introduction of an "internal solvent"[13] is well known and used within the classical liquid-crystal community.

The addition of surfactants to inorganic clusters as their counterions usually results in crystalline materials.[14, 15] For the lanthanide alkanoates the properties of the lanthanide counterion were critical for the formation of organized structures in these systems.[16] For the silver-containing polycatenar materials, for which the addition of silver dodecylsulfate to a stilbazole precursor leads to the formation of the final polycatenar material, both thermotropic[17] and lyotropic[18] phase behavior have been observed. Mesostructured materials with long-range order based on clusters and surfactants were also obtained from the addition of surfactants to polyoxometalates (hollow/spherical and ring-shaped clusters); however (except in case of the macrorings), the materials only displayed surfactant-encapsulated structures.[19, 20, 21] These materials are analogous to the known organic polyelectrolyte–surfactant materials,[22] where the addition of charged surfactants to an oppositely charged polyelectrolyte leads to the formation of mesostructured materials in a highly cooperative manner. The direct translation into inorganic polyelectrolyte–surfactant complexes has also been reported.[23]

Herein we employ the ISA route to generate nanostructured organic/inorganic hybrid materials with switchable structures from a special inorganic oligoelectrolyte species, the trimetallic concave cyclic anion $[Ni_3P_3S_{12}]^{3-}$ (**1**) with pseudo-C_{3v} symmetry. This species is obtained from the autofragmentation/rearrangement of the inorganic polymer $^1_\infty[NiPS_4]^-$ in dimethylformamide (DMF) at 50 °C.[24] The synthesis[25, 26] and properties[24, 27] of the polymer are descri-

[a] Dr. C. F. J Faul, Dr. F. Camerel, Prof. Dr. M. Antonietti
Max Planck Institute of Colloids and Interfaces
Research Campus Golm, 14424 Potsdam-Golm (Germany)
Fax: (+49) 331-567-9502
E-mail: Charl.Faul@mpikg-golm.mpg.de

DOI: 10.1002/chem.200204528

bed in detail elsewhere. This bowl-shaped cyclic anion **1**, whose charges are mainly localized on the three single-bonded outer sulfur atoms,[27] appears to be a good candidate to form mesophases by the ISA route with charged surfactants. This notion is supported by the tendency of this crown of pseudo-C_{3v} symmetry to form 1D or 2D crystalline arrangements after exchange of the alkali cations by small organic cations.[28]

Results and Discussion

A series of double-tail dialkyldimethylammonium surfactants ($DiC_{12}DAB$, $DiC_{14}DAB$, $DiC_{16}DAB$, and $DiC_{18}DAB$) was selected for complexation with the potassium salt of the oligoelectrolytic crown **1**. These surfactants were chosen with the aim of producing soft, mesostructured noncrystalline materials, as deduced from our previous work. The surfactants were dissolved in DMF, and added to **1** in a 3:1 ratio (stoichiometric in terms of charges). No precipitation occurred, but flexible red films were obtained after evaporation of the solvent. Wide-angle X-ray scattering (WAXS) analyses confirmed the formation of KBr crystals as the side product of the complexation process. Direct removal of the resulting salt by extraction with water could not be performed, since the P–S bonds in thiophosphate compounds are susceptible to hydrolysis in aqueous media. However, the crown (now surrounded by long-chain surfactants) can easily be separated (by extraction with organic solvents such as chloroform or toluene) from the salts. WAXS analyses underlined both the absence of KBr in the films (vacuum-dried again) and that they were noncrystalline. Energy-dispersive X-ray analyses (EDAX) analyses on these films showed only the presence of Ni, P, and S. No K or Br could be detected, which confirmed the complete and cooperative exchange of the small cation with the dialkyldimethylammonium species. The 3:1 ratio of complexation was also confirmed by means of elemental analyses.

The films were investigated by polarized optical microscopy and exhibited strong birefringence (Figure 1). This clearly pointed to the fact that these materials are thermotropic liquid crystals at room temperature (WAXS analyses, see above, already showed that the films are noncrystalline). No typical textures could be identified and no additional information could be obtained from the color.

The thermal properties of these materials were investigated by thermogravimetric analysis (TGA) and differential scanning calorimetry (DSC). TGA analyses revealed that the degradation temperature was generally above 220 °C. DSC analyses showed that, except for the $DiC_{12}DA$ complex, all others exhibit reversible thermal transitions. Figure 2 shows, as an example, the DSC curve of the $[Ni_3P_3S_{12}]^{3-}/DiC_{16}DA$ complex. A strong endothermic transition ($\Delta H = 9.0\ J\,g^{-1}$) is found centered around 24.3 °C, with some precursor melting due to less-ordered domains. As the length of the alkyl tail increases (from DiC_{14} to DiC_{18}), the transition temperatures and transition enthalpies for this transition also increase. This is why we attribute this transition to structural rearrangements of the side chains rather than to to major phase changes

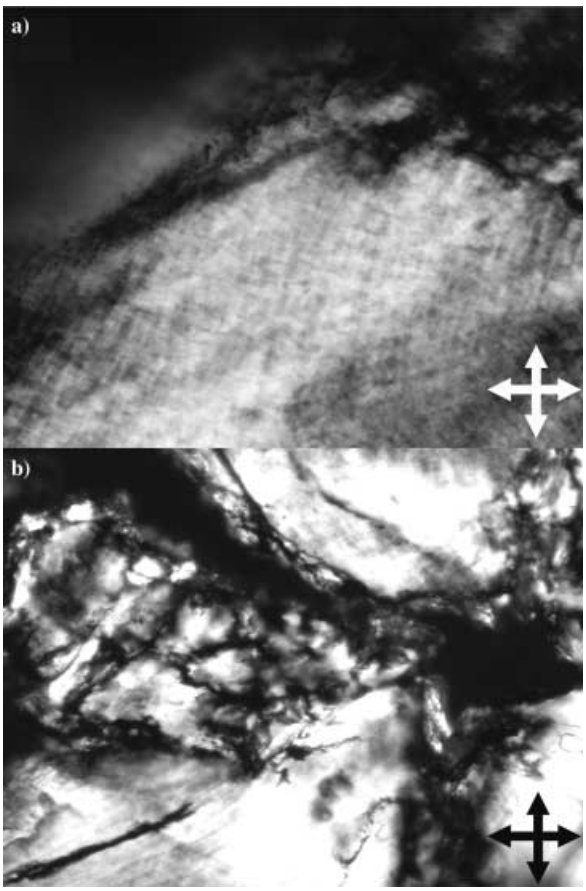

Figure 1. Inorganic cluster/surfactant composites viewed by optical microscopy under crossed polarizers (symbolized by the cross in the corner of the picture); a) $[Ni_3P_3S_{12}]^{3-}/DiC_{12}DA$ complex at room temperature; b) $[Ni_3P_3S_{12}]^{3-}/DiC_{14}DA$ complex at 100 °C.

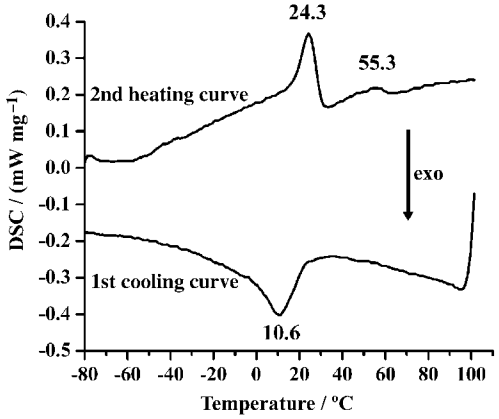

Figure 2. DSC curve of the $[Ni_3P_3S_{12}]^{3-}/DiC_{16}DA$ film.

of the clusters. A second, weaker transition ($\Delta H = 1.8\ J\,g^{-1}$) occurs at 55 °C, which is more pronounced in the first heating cycle, indicating that it is either an effect which relies on tempering and slower ordering processes or even an irreversible transition.

To elucidate the morphology of these mesostructured materials, a range of temperature-dependent WAXS and SAXS measurements was performed. In all cases WAXS analyses showed no reflections in the wide-angle region, and only a broad reflection at approximately 20° (*d* spacing

$\sim$0.45 nm). This is indicative of a liquidlike arrangement of alkyl tails.

Room-temperature SAXS analysis of the $[Ni_3P_3S_{12}]^{3-}$/$DiC_{14}DA$ complex showed that some type of phase coexistence was present in the as-prepared samples, since the well-developed scattering peaks could be indexed according to two different sets (see Figure 3a). Since several transitions were present in the DSC curve below 100 °C, a SAXS diffractogram was also recorded at this temperature. The resulting diffractogram showed the presence of one lamellar phase only, with a *d* spacing of 2.39 nm. An interesting feature present in this diffractogram as well as in those of all the other complexes except for the $DiC_{12}DA$ crown complex at room temperature, is the broad peak found at an *s* value of approximately 1.25 nm^{-1}. The exact origin of this reflection will be discussed in more detail below.

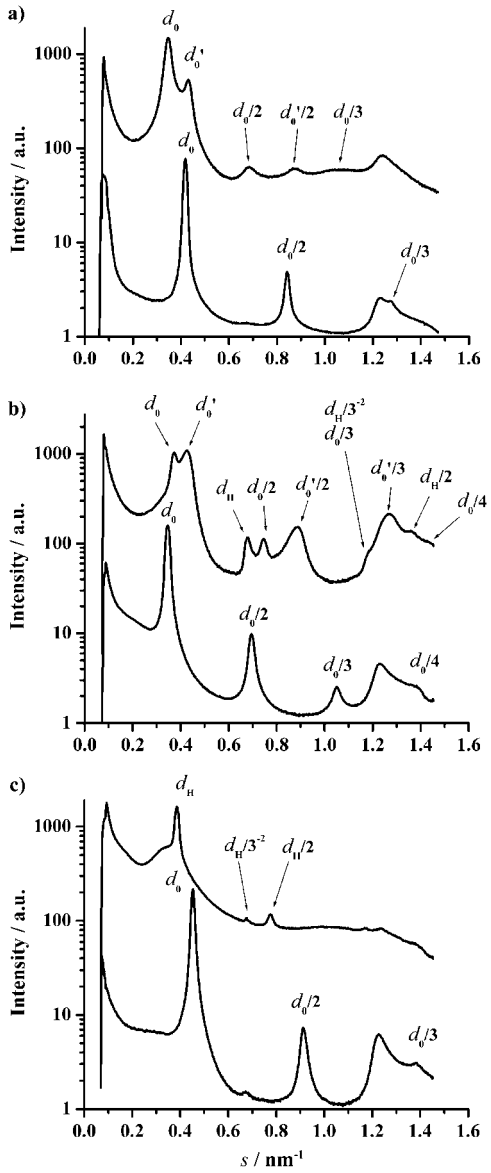

Figure 3. a) SAXS data of the $[Ni_3P_3S_{12}]^{3-}$/$DiC_{14}DA$ complex; b) the $[Ni_3P_3S_{12}]^{3-}$/$DiC_{16}DA$ complex; and c) the $[Ni_3P_3S_{12}]^{3-}$/$DiC_{12}DA$ complex at room temperature (top curve) and 100 °C (bottom curve).

Very similar results to that of the $DiC_{14}DA$ complex were obtained for the $DiC_{18}DA$ complex. SAXS analysis of this complex also showed phase coexistence at room temperature, presumably of two lamellar phases. The diffractogram recorded at 100 °C once again showed that only one lamellar phase with a *d* spacing of 3.09 nm was present.

Room-temperature SAXS analysis of the $[Ni_3P_3S_{12}]^{3-}$/$DiC_{16}DA$ complex yielded an even more complex diffraction pattern consisting of one lamellar and another lamellar/hexagonal phase (Figure 3b). Heating the sample to 100 °C (past all transitions according to the DSC analysis) led to a rearrangement and the disappearance of the phases present at room temperature. Here, only one lamellar phase (*d* spacing = 2.89 nm) with well developed and characteristic reflections at ratios of 1:2:3:4 (Figure 3b) is observed. The characteristic broad reflection at $s \approx 1.25$ nm^{-1} was present in all recorded diffractograms.

In the case of the $[Ni_3P_3S_{12}]^{3-}$/$DiC_{12}DA$ complex, the influence of the shorter alkyl tails on the phase structure was evidenced by the fact that the initial phase found at room temperature was an hexagonal phase (Figure 3c) with no other phase coexisting. If the dimensions of the inorganic crown (the thickness and diameter of which were calculated to be approximately 0.6 nm and approximately 1.4 nm, respectively) and the length of the stretched alkyl chains are taken into consideration (Table 1), this hexagonal phase can be explained by a columnar phase of crowns embedded in a matrix of alkyl tails. Interestingly, the broad reflection at $s \sim 1.25$ nm^{-1} (observed in all other samples) is not present in the hexagonal phase. Even though the DSC curves of the complex showed no transitions, a SAXS diffractogram was recorded at 100 °C. Here, the characteristic 1:2:3 pattern of a lamellar phase (*d* spacing = 2.21 nm) and the characteristic broad reflection at $s = 1.25$ nm^{-1} now also appeared for the DiC_{12} species. A further SAXS measurement, after cooling the sample down from 100 °C to −80 °C and slowly leaving to heat up to room temperature again, showed that the lamellar phase and the broad reflection were preserved.

For all complexes it is however worth mentioning that the period repeat unit of the high-temperature phase is significantly smaller than that of the original low-temperature phase. This is somewhat unexpected and directly related to a better distribution of the inorganic material in the organic matrix. Since the crown (complexed by the surfactants) is shaped as a discotic tectonic unit, we were expecting to find

Table 1. Dimensions of the stretched alkyl chains (l_{chain}), *d* spacing found from the SAXS patterns at room temperature and at 100 °C, and length of the whole surfactant (l_{surf} including the dimethylammonium head group) in nm.[a]

	l_{chain}	*d* spacing	l_{surf}
$DiC_{12}DAB$	1.67	2.59 Hex (RT) 2.21 Lam (100)	2.07
$DiC_{14}DAB$	1.92	2.88 Lam; 2.39 Lam (RT) 2.39 Lam (100)	2.32
$DiC_{16}DAB$	2.18	2.68 Lam; 2.34 Lam; 1.47 Hex (RT),2.89 Lam (100)	2.58
$DiC_{18}DAB$	2.43	2.86 Lam, 2.74 Lam (RT) 3.09 Lam (100)	2.83

[a] The maximum length of the dimethylammonium head group was estimated to be 0.4 nm from X-ray crystal structures containing alkylammonium head groups (N–C $\sim$0.15 nm; C–H $\sim$0.1 nm).

columnar phases. This was however only seen for the $DiC_{12}DA$–crown complex. The maximum length of the alkyl chains as well as the *d* spacing found from SAXS results are shown in Table 1. Keeping the size of the crown species and the length of the alkyl tails in mind, it is noted that the repeat distances in all cases (lamellar and hexagonal phases) are comparably small.

The coexistence of phases, the phase changes observed, and approximate calculations of size reveal that the crown species is not necessarily still intact within the solid films. Chemical changes inside the film are also supported by the fact that for the $DiC_{12}DA$–crown complex, a phase change is observed at 100 °C (by SAXS analyses) without any transition present in the DSC curve. As both the original inorganic polymer and the crown species have very distinct UV spectra, it was therefore decided to check for the presence of the crown species by UV spectroscopy. UV spectra were recorded from samples spin-coated onto quartz slides and then treated at the same temperatures as for the bulk films. In addition, UV solution spectra were measured immediately after dissolution of the films in DMF.

The results obtained from UV measurements are summarized in Figure 4. In all the cases, except for the $[Ni_3P_3S_{12}]^{3-}$/$DiC_{12}DA$ complex at room temperature, all of the films contained, in addition to the crown species ($\lambda_{max} = 305$ nm), inorganic polyelectrolyte ($\lambda_{max} = 370$ nm) as well. After the sample was heated to 100 °C, the band attributed to the inorganic polyelectrolyte at 370 nm was much more pronounced, and even appeared in the UV spectra of the $DiC_{12}DA$–crown system (Figure 4b). This is contrary to what

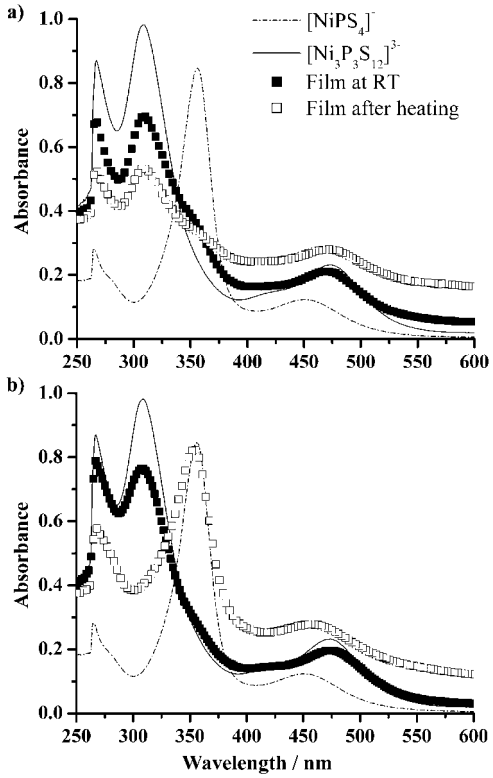

Figure 4. UV/Vis spectra of the $DiC_{16}DA$ (a) and the $DiC_{12}DA$ (b) films at room temperature and after heating to 100 °C in DMF.

is expected, since heating in solution always leads to the reversed process, that is fragmentation of the polymer to the crown.

Tests on the stability of the pure inorganic materials revealed that heating the polymer or the crown in the solid state to a temperature above 150 °C led to no change in the molecular composition, that is this transition is indeed purely structural. UV spectra of a corresponding low molecular weight salt, namely $(PPh_4^+)_3[Ni_3P_3S_{12}]^{3-}$ crystals, in the solid state and in solution, were recorded before and after heating. No formation of polymer was observed. However, removal of the solvent from a suspension of the $(K^+)_3[Ni_3P_3S_{12}]^{3-}$ salt (in DMF) led to the formation of polymer in the dry state. The stability of these amorphous films in air is however very low compared to that of the polymer/surfactant films.

All these experiments show that the polymerization in the soft solid state is presumably induced by the close proximity and favorable mutual arrangement of the single crown species, and that it is possible to control this polymerization process in the self-assembled liquid-crystalline state. It was also found that the polymerization process in the solid state is irreversible, and that the composition of the films does not change after several months of storage in air, (i.e. no degradation). Another interesting observation made during the UV investigations in solution was the following: when samples were dissolved in DMF after heating, and the spectrum recorded immediately after dissolution was compared to one taken after 24 h of stirring, no polymer could be detected in the UV trace of the stirred sample. Evidently, the alkyl chains did not stabilize the polymer chains in DMF solution against the autofragmentation and rearrangement reactions known for the polymer. When films were then cast again (i.e. after stirring), as, for example, in the case of the $DiC_{12}DA$ complex, the films exhibited the initial hexagonal phase structure in a reversible way.

To confirm the switch between crown and polymer in these materials, we studied the system showing the most marked changes, that is the $[Ni_3P_3S_{12}]^{3-}$/$DiC_{12}DA$ system by ^{31}P NMR spectroscopy (see reference [24] and [27] for more details). Solution-state ^{31}P NMR spectra were recorded on freshly prepared deuterated DMF solutions from freshly prepared inorganic materials, and from the same materials heated to and kept at 100 °C for 4 h. Short acquisition times were used to ensure exclusion, as far as possible, of all possible degradation reactions and of formation of side products. It is known that the polymer species shows a signal at $\delta = 123$ ppm; a signal from the crown species gradually appears at $\delta = 114$ ppm as the autofragmentation and rearrangement takes place. Spectra obtained from the $[Ni_3P_3S_{12}]^{3-}$/$DiC_{12}DA$ complex film cast in chloroform at room temperature (Figure 5a) display only one peak at $\delta = 113.7$ ppm confirming the presence of mainly the crown species in this complex. Spectra obtained of the same films after heating at 100 °C (in DMF, recorded immediately after dissolution) display only one peak at $\delta =$ 122.7 ppm (Figure 5b), characteristic of the polymer in DMF. These results confirm the UV/Vis observations and the complete repolymerization in the soft solid state. After several hours, this signal in DMF gradually disappears and the signal of the crown gradually appears at $\delta = 114$ ppm as

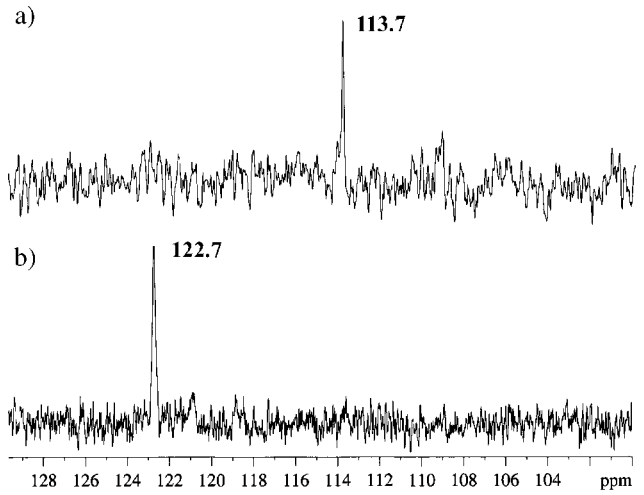

Figure 5. Solution-state ^{31}P NMR spectra at 273 K of a) a freshly prepared $[Ni_3P_3S_{12}]^{3-}/DiC_{12}DA$ complex film dissolved in DMF and b) of the same film dissolved in DMF after heating at 100 °C for 4 h.

the fragmentation process takes place again. Temperature-dependent solid-state ^{31}P NMR experiments were also performed on the solid films. Owing to the high dilution of the signals of the nonequivalent phosphorus atoms of the crown in these solid materials, no clear spectra showing the crown could be obtained. However, during measurements at 100 °C the signal of the polymer at $\delta \approx 123$ ppm was observed, and was retained after cooling to room temperature. These results confirm the stabilization of the polymer in the liquid-crystalline state.

The described process also has to be discussed within the broader framework of polymerization reactions within organized and mesostructured soft systems, a theme that has been under investigation for several years.[29, 30] Usually, polymerization of the included species either leads to disruption of the structure-directing phase,[31] which is due to minor enthalpic and very large entropic changes throughout the polymerization reaction, or in favorable cases, to anisotropic nanostructured networks[32] or anisotropic polymeric nanoparticles with a structure different from the primary phase.[33] Recently we have made use of polyaddition reactions within mesostructured polyelectrolyte–surfactant complexes to produce a fixed, one-to-one copy of the original mesophasic structure.[34] The presently described well-defined structural transition is therefore a rare case, underlining the high definition and flexibility of organic/inorganic ISA hybrid materials.

It also became clear that the length of the alkyl chains, and therefore the material properties of the formed complex (such as packing parameters, viscosity, and phase transitions), play an important role in the structure of the films and the onset of the structural transitions. In the case of the shortest alkyl tail, the $DiC_{12}DA$ system, stabilization of the crown in the solid state is at a maximum. After heating to 100 °C, the inorganic polyelectrolyte is formed with the accompanying phase change, and was still present when the sample was cooled back to room temperature. This was not a classical thermotropic phase transition as was expected at first, but rather a permanent phase change due to heating, as might be applied in data storage applications. The structural transition is nevertheless reversible, involving a solvent/dissolution cycle.

For the other three systems, there was a gradual decrease in the stabilization of the crown within the alkyl matrix, which is presumably driven by an altered liquid-crystalline phase structure. The presence of mixed lamellar phases after the initial casting of the films (with even a hexagonal phase present in the $[Ni_3P_3S_{12}]^{3-}/DiC_{16}DA$ system) can now be explained in terms of a mixture of polymer and crown inorganic subphases, which result in the coexistence of more than one phase to accommodate the different species (with the crowns also presumably being arranged in a lamellar discotic phase). With heating, sufficient polymer is formed to produce a single lamellar phase. In the case of $[Ni_3P_3S_{12}]^{3-}/DiC_{16}DA$, the existence of both hexagonal and lamellar sets of scattering peaks is presumably attributed to an ordered hexagonal arrangement of the crown species within the lamellar subphase, that is a smectic B type arrangement. The calculated unit cell parameter for the hexagonal substructure is $a = 1.70$ nm (from $d = 1/s = (\sqrt{3} \times a/2)$, which is much smaller than the hexagonal structure of the $[Ni_3P_3S_{12}]^{3-}/DiC_{12}DA$ system. This underlines the fact that for the larger tails, the surfactants are not between the crowns, but rather allocated perpendicular to the crown plane in a different subphase.

The additional broad reflection at $s \sim 1.25$ nm^{-1} thus originates from the polymer chains, since it was not found (or to a very low degree only) in the materials where no polymer ($DiC_{12}DA$ system) was present. From the known dimensions of the polymer (diameter ca. 0.67 nm), we suggest that this peak is most probably due to interchain contributions, that is the Ni sites adopt a certain regularity within the lamellar plane of the inorganic subphase. The absence of any reflection at $s \sim 1.25$ nm^{-1} (0.8 nm repeat distance) in the WAXS of the pure polymer confirms that this reflection does not have an intrachain origin.

The Pd-containing polymer, in contrast to the Ni-containing polymer used throughout this investigation, is slightly more stable in DMF up to temperatures of 70 °C (a cooperative fragmentation and degradation process start at this temperature). To perform comparative investigations with polymer species only, we also synthesized complexes from the Pd-analogue polymer with charged double-tail dialkyldimethylammonium surfactants. However, this led to the formation of less-ordered materials, as evident from the broad peaks in the SAXS region only. This indicates that the organization of polymer species into very highly ordered materials is more favorably done by the self-assembly of the precursors followed by in situ solid-state polymerization in the ordered structure.

Finally, TEM experiments were performed on dried samples from solutions of the crown–surfactant complexes. Figure 6 shows an electron micrograph of a thin film obtained by depositing a freshly prepared solution of the $[Ni_3P_3S_{12}]^{3-}/DiC_{12}DA$ complex in chloroform at room temperature. On this TEM image, one can clearly observe parallel lines with a lattice spacing of 2.29 nm. This value is close to that of the lamellar spacing (2.21 nm) of the solid-state structure of this

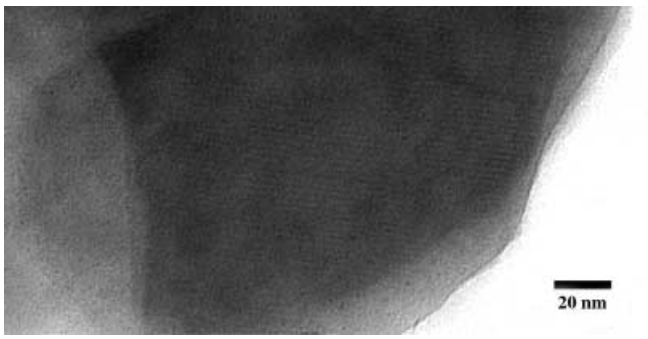

Figure 6. TEM image of the $[Ni_3P_3S_{12}]^{3-}/DiC_{12}DA$ complex deposited on a perforated carbon-film copper grid from chloroform at room temperature.

complex observed after heating. Thus, the observed organized thin-layer structure is presumably attributed to a polymerized structure, which is induced by the heat and electron uptake from the electron beam. We were not able to observe any indications of the primary hexagonal structure by TEM. Again, this indicates the potential of such materials for recording and structuring purposes by electron beam writing.

Conclusion

In conclusion, we have shown that it is possible to produce stable, room-temperature liquid-crystalline materials by ionic self-assembly, that is electrostatic coupling of anisotropic inorganic clusters with charged double-tail dialkyldimethylammonium surfactants. The materials produced from the inorganic crown $[Ni_3P_3S_{12}]^{3-}$ together with the alkyl chains, which serve as an internal solvent, show interesting phase and thermal polymerization behavior in the soft solid state. Furthermore, the reversible two-state switchability of this system was demonstrated for the $[Ni_3P_3S_{12}]^{3-}/DiC_{12}DA$ complex, for which a reversible change from crown to polymer (by heat) and back to the crown species (by solvent) was demonstrated.

In addition, an original smectic B type discotic arrangement was observed for the $DiC_{16}DA/[Ni_3P_3S_{12}]$ complex, for which the inorganic tectonic unit is ordered in a hexagonal 2D array inside a lamellar subphase. The formation of unusually highly ordered lamellar polymer phases at 100 °C shows that organization of polymers into highly ordered materials can preferentially be achieved by a self-assembly of the precursors followed by the in situ solid-state polymerization where polymerization and ordering occur simultaneously and mutually depend on each other.

Similar studies are currently in progress to determine the capability of these materials to respond to pressure instead of temperature. We also assume that these materials have some potential for data storage and the creation of surface nanostructures by either optical or electron-beam writing.

Experimental Section

$KMPS_4$ compounds (M = Pd or Ni) were synthesized as described elsewhere.[25, 26] A dark brown solution of the $[Ni_3P_3S_{12}]^{3-}$ crown was obtained after dissolution of fine crystals of $KNiPS_4$ in DMF (65.5 mmol L^{-1}) and heating for one week at 50 °C under stirring.[24] Insoluble components were removed by filtration. Stoichiometric amounts (1:1 charge ratio) of the cationic double-tail alkylammonium bromide surfactants (Aldrich), dissolved in a minimum of DMF, were added to solutions of $K_3[Ni_3P_3S_{12}]$. The solutions were stirred for one hour after addition of the surfactant. A large part of the KBr was removed by precipitation after addition of diethyl ether and filtration. Evaporation of the solvents (diethyl ether + DMF) at room temperature under low pressure led to the formation of dark brown films. The integrity of the crown in this film was confirmed by UV/Vis spectroscopy. This film was then redissolved in chloroform, filtered, and quickly extracted with a small amount of water to insure the removal of residual potassium salts. After casting in a Teflon-coated aluminum holder (BYTAC, Fisher), a dark brown film is obtained after evaporation. The films were dried under vacuum (50 mbar) at room temperature. EDAX and WAXS measurements confirmed the removal of the potassium salts. Elemental analysis (N, S) indicated that the 1:1 charge ratio of complexation was fulfilled and excluded the presence of free surfactant or uncomplexed inorganic cluster in the solid precipitate. $(PPh_4)_3[Ni_3P_3S_{12}]$ crystals were synthesized as described elsewhere[24] as a reference compound.

Elemental analyses (C, H, N, S) were performed on a Vario EL Elementar (Elementar Analysen-systeme, Hanau, Germany). Differential scanning calorimetry (DSC) was performed on a Netzsch DSC 200. The samples were examined at a scanning rate of 10 K min^{-1} by applying two heating and one cooling cycle. Thermogravimetric analyses were performed on a Netzsch TG 209. The samples were examined at a scanning rate of 20 K min^{-1} from room temperature to 300 °C.

Small-angle X-ray scattering measurements were carried out with a Nonius rotating anode ($U = 40$ kV, $I = 100$ mA, $\lambda = 0.154$ nm) using image plates. With the image plates placed at a distance of 40 cm from the sample, a scattering vector range of $s = 0.07 - 1.6$ nm^{-1} was available. The 2D diffraction patterns were transformed into 1D radial averages. The data noise was calculated according to Poisson statistics, which is a valid approach for scattering experiments. WAXS measurements were performed by using a Nonius PDS120 powder diffractometer in transmission geometry. A FR590 generator was used as the source of $Cu_{K\alpha}$ radiation ($\lambda = 0.154$ nm). Monochromatization of the primary beam was achieved by means of a curved Ge crystal. Scattered radiation was measured by using a Nonius CPS120 position-sensitive detector. The resolution of this detector in 2θ is 0.018 °.

UV/Vis spectra were recorded using a UVIKON 940/941 dual-beam grating spectrophotometer (Kontron Instruments) with a 1 cm quartz cell. Solution-state ^{31}P NMR spectra were recorded on a Brucker DPX400 spectrometer operating at a frequency of 161.982 MHz. Spectra were collected with a 30 ° pulse length of ~7.8 μs and a power level of 0 dB and a recycle time of 5 s. Processing of the data was performed by using the XWINPLOT (Brucker) program. The measurement were performed on deuterated DMF solutions at a concentration of about 10^{-3} mol L^{-1} (low concentrations were used to ensure a fast dissolution of the species). Spectra were collected with a good signal/noise ratio after 45 min. ^{31}P solid-state MAS-NMR spectra were recorded at 161.808 MHz on a Brucker DMX400 solid-state NMR spectrometer. Spectra were collected with a 90 ° pulse of 4 μs, a power level of 2 dB, and a recycle time of 5 s. ^{31}P NMR chemical shifts were referenced through an external 85 % aqueous solution of H_3PO_4 at 0 ppm and proton decoupling was used.

Transmission electron microscopy (TEM) images were acquired on a Zeiss EM912W instrument at an acceleration voltage of 120 kV by depositing a 5 μL drop of a suspension of the composite material in chloroform onto a perforated carbon-film covered grid. Energy-dispersive X-ray analysis (EDX) experiments were performed on an EDAX-equipped LEO Gemini 1530 scanning electron microscope.

Acknowledgement

We thank the Max Planck Society and the Fund of the German Chemical Industry for financial support. We gratefully acknowledge help with the X-ray measurements by Ingrid Zenke, with the NMR measurements by Olaf Niemeyer, with the TEM experiments by Rona Pitschke and Dr. Jürgen Hartmann, and technical help by Carmen Remde.

[1] A. Klug, *Angew. Chem.* **1983**, *95*, 579; *Angew. Chem. Int. Ed. Engl.* **1983**, *22*, 565 – 582.
[2] C. L. Brooks, M. Karplus, B. M. Pettitt, *Proteins: A Theoretical Perspective of Dynamics, Structure and Thermodynamics*, Wiley, New York **1986**.
[3] J. M. Lehn, *Supramolecular Chemistry: Concepts and Perspectives*, VCH, Weinheim **1995**.
[4] L. A. Cuccia, E. Ruiz, J-M. Lehn, J-C. Homo, M. Schmutz, *Chem. Eur. J.* **2002**, *8*, 3448 – 3457.
[5] E. R. Zubarev, M. U. Pralle, E. D. Sone, S. I. Stupp, *Adv. Mater.* **2002**, *14*, 198 – 203.
[6] O. Ikkala, G. ten Brinke, *Science* **2002**, *295*, 2407 – 2409.
[7] J.-M Lehn, *Proc. Natl. Acad. Sci. USA* **2002**, *99*, 4763 – 4768.
[8] S. Fernandez-Lopez, H-S. Kim, E. C. Choi, M. Delgado, J. R. Granja, A. Khasanov, K. Kraehenbuehl, G. Long, D. A. Weinberger, K. M. Wilcoxen, M. R. Ghadiri, *Nature* **2001**, *412*, 452 – 455.
[9] C. F. J. Faul, M. Antonietti, *Chem. Eur. J.* **2002**, *8*, 2764 – 2768
[10] C. T. Seto, G. M. Whitesides, *J. Am. Chem. Soc.* **1990**, *112*, 6409 – 6411.
[11] M. T. Youinou, N. Rahmouni, J. Fischer, J. A. Osborn, *Angew. Chem.* **1992**, *104*, 771 – 773; *Angew. Chem. Int. Ed. Engl.* **1992**, *31*, 733 – 735.
[12] Y. Guan, M. Antonietti, C. F. J. Faul, *Langmuir* **2002**, *18*, 5939 – 5945.
[13] S. Chandrasekhar, B. K. Sadashiva, K. A. Suresh, *Pramana* **1977**, *9*, 471 – 480.
[14] M. Wachhold, M. Kanatzidis, *Chem. Mater.* **2000**, *12*, 2914 – 2923.
[15] G. G. Janauer, A. D. Dobley, P. Y. Zavalij, M. S. Whittingham, *Chem. Mater.* **1997**, *9*, 647 – 649.
[16] K. Binnemans, L. Jongen, C. Görlerr-Walrand, W. D′Olieslager, D. Hinz, G. Meyer, *Eur. J. Inorg. Chem.* **2000**, *7*, 1429 – 1436.
[17] B. Donnoi, B. Heinrich, T. Gulik-Krzywicki, H. Delacroix, D. Guillon, D. W. Bruce, *Chem. Mater.* **1997**, *9*, 2951 – 2965.
[18] A. I. Smirnova, D. W. Bruce, *Chem. Commun.* **2002**, 176 – 177.
[19] D. G. Kurth, P. Lehmann, D. Volkmer, H. Cölfen, M. J. Koop, A. Müller, A. Du Chesne, *Chem. Eur. J.* **2000**, *6*, 385 – 393.
[20] S. Polarz, B. Smarsly, M. Antonietti, *Chem. Phys. Chem.* **2001**, *7*, 457 – 461.
[21] D. Volkmer, A. Du Chesne, D. G. Kurth, H. Schnablegger, P. Lehmann, M. J. Koop, A. Müller, *J. Am. Chem. Soc.* **2000**, *122*, 1995 – 1998.
[22] M. Antonietti, J. Conrad, A. Thunemann, *Macromolecules* **1994**, *27*, 6007 – 6011.
[23] B. Messer, J. H. Song, M. Huang, Y. Wu, F. Kim, P. Yang, *Adv. Mater.* **2000**, *12*, 1526 – 1528.
[24] J. Sayettat, L. M. Bull, J.-C. P. Gabriel, S. Jobic, F. Camerel, A.-M. Marie, M. Fourmigué, P. Batail, R. Brec, R.-L. Inglebert, *Angew. Chem.* **1998**, *110*, 1773 – 1776; *Angew. Chem. Int. Ed.* **1998**, *37*, 1711 – 1714.
[25] S. H. Elder, A. Van der Lee, R. Brec, E. Canadell, *J. Solid State Chem.* **1995**, *116*, 107 – 112.
[26] K. Chondroudis, M. G. Kanatzidis, J. Sayettat, S. Jobic, R. Brec, *Inorg. Chem.* **1997**, *36*, 5859 – 5868.
[27] J. Sayettat, L. M. Bull, S. Jobic, J.-C. P. Gabriel, M. Fourmigué, P. Batail, R. Brec, R.-L. Inglebert, C. Sourisseau, *J. Mater. Chem.* **1999**, 9, 143 – 153.
[28] M. Bujoli-Doeuff, S. Coste, M. Evain, R. Brec, D. Massiot, S. Jobic, *New J. Chem*. **2002**, *26*, 910 – 914.
[29] *Polymerization in Organised Media* (Ed.: C. M. Paleos) Gordon Breach Science Publishers, Philadelphia **1994**.
[30] H.-P. Hentze, M. Antonietti, *Curr. Opin. Solid State Mater. Sci.* **2001**, *5*, 343 – 353.
[31] M. Antonietti, H.-P. Hentze, *Colloid. Polym. Sci.* **1996**, *274*, 696 – 702.
[32] M. Antonietti, C. G. Göltner, H.-P. Hentze, *Langmuir* **1998**, *14*, 2670 – 2676
[33] C. F. J. Faul, M. Antonietti, R. D. Sanderson, H.-P. Hentze, *Langmuir* **2001**, *17*, 2031 – 2035.
[34] D. Ganeva, C. F. J. Faul, C. Götz, R. D. Sanderson, *Macromolecules,* **2003**, in press.

Received: October 24, 2002 [F4528]

